PROCEEDINGS

OF THE

SIXTH SYMPOSIUM

ON THE

GEOLOGY OF THE BAHAMAS

Edited by

Brian White

Production Editor

Donald T. Gerace

Bahamian Field Station
San Salvador, Bahamas
1993

Printed in USA by Don Heuer

ISBN 0-935909-43-5

DOLOMITIZATION BY SALINE GROUND WATERS WITHIN THE NORTH-WESTERN GREAT BAHAMA BANK: AN OVERVIEW.

Fiona F. Whitaker and Peter L. Smart
Department of Geography
University of Bristol
Bristol BS8 1SS
England

ABSTRACT

Measurements of salinity, temperature and ground water discharges within the Great Bahama Bank provide evidence for active circulation of large volumes of near-normal ocean water beneath Andros Island, Bahamas. Slightly elevated salinity waters (38-42‰) derived from the Great Bahama Bank flow eastwards beneath the island, and mix with normal salinity cold ground waters (19-20°C) from deeper than 250 m in the adjacent oceans. Volumetric budgeting of saline discharges along the east coast of North Andros suggest an average flow rate of 2.9 to 35 x 10^{-2} m/d. Circulation of bank waters appears to be driven by reflux of only slightly elevated salinity waters as suggested by Simms (1984), while sea water circulation occurs by thermally-driven Kohout convection and/or in response to trans-island/bank differences in sea surface elevation.

Saline ground water sampled in inland blue holes and at discharge sites on the east coast have an elevated PCO_2, lower SI_C and are depleted in sulphate by up to 5% compared to sea water. Furthermore, these waters are depleted in magnesium and enriched in calcium relative to open ocean and bank input waters. Replacement dolomitization of low-magnesium calcite by these waters therefore appears to be occuring under conditions of elevated carbonate activity and is progressive along the flow path. Combination of estimated ground water flux with an average magnesium depletion of 67 mg/L indicates dolomitisation occurs at an approximate rate of 1.8 to 22 x 10^{-6} %/a.

Sparse micro-dolomites and dolomitic cements occur in wall rock samples from the zone of saline ground water in Stargate Blue Hole, South Andros. Four types of dolomites are recognised: isolated rhombs of 4-5 μm, patches of anhedral crystals of 30-50μm, fabric selective replacement of allochems, and rim cements. Strontium isotopes yield a maximum age of 0.4-0.8 Ma for the dolomite, substantially younger than the host rock (1.5-2.5 Ma). Stable and trace element analyses suggest precipitation from cold near-normal sea water under slightly reducing conditions. The current rate of dolomitisation, estimated from aqueous geochemical and ground water flow measurements, combined with subsidence rates and sea-level history are sufficient to account for the observed concentrations of dolomite in wall-rock samples.

INTRODUCTION

Modern dolomites have been reported forming in a variety of different environments, including supra-tidal flats, sabkhas and deep-sea sediments, and have provided new insights into the geochemical processes controlling dolomitisation. However, these dolomites are not analogous to the thick sequences of Late Cenozoic dolomites which occur at relatively shallow depth throughout the Bahamas. These replacement dolomites appear to have formed at near surface temperatures and pressures and are not associated with evidence of evaporitic conditions (Dawans and Swart, 1988; Vahrenkamp and Swart, in press). Following Badiozamani (1973) dolomitisation in the fresh-salt water mixing zone became widely accepted to explain these types of dolomites (Dawan and Swart, 1988), but increasingly this paradigm has been questioned because of the restricted vertical extent of this zone, and apparent absence of dolomites in modern mixing zones (Machel and Mountjoy, 1986). More recently, therefore, attention has focused on the potential for dolomitisation by sea water (Land, 1985).

In this paper we present an overview summarising our work on dolomitisation by saline ground waters circulating through the north-western Great Bahama Bank beneath Andros Island. The approach adopted uses oceanic and inland blue holes to access the interior of the Bank and combines study of the ground water circulation (Whitaker and Smart, 1990; Whitaker and Smart, in press) with aqueous geochemistry and sampling of shallow dolomites (Whitaker *et al.*, in press). The paper is divided into

3 main sections; first we present field evidence of large-scale circulation of bank and open ocean sea waters through the Great Bahama Bank; second we examine the geochemistry of these waters and suggest magnesium depletion in them is caused by replacement dolomitisation; and finally we describe sparse replacement dolomites from shallow depth in the saline zone, the geochemistry and probable age of which is compatible with our aqueous geochemical and hydrological observations.

HYDROLOGY OF SALINE GROUND WATERS

Methods

Oceanic blue holes along the east coast of Andros Island are characterised by strong semi-diunally reversing currents that develop in response to variations in local tidal head. In order to differentiate between this shuttling of locally derived sea-water and any larger-scale net saline ground water circulation, continuous monitoring was undertaken using Aanderaa oceanographic recording current meters (RCMs). These instruments were operated in Rat Cay and South Mastic oceanic blue holes on the east coast of North Andros (Figure 1), and record flow velocity and direction, salinity, temperature and local tidal head. Point velocities derived from the RCM record were converted to average velocity using *in situ* measurements of the cross-sectional velocity distribution throughout the tidal cycle obtained by divers using hand-held current meters. Discharge was then calculated using this average velocity and the surveyed cross sectional area of the passage.

Salinity and temperature were used as natural tracers of saline ground water source and flow path. Salinity and temperature were measured *in situ* to a maximum depth of 100 m in 27 deep inland cenote blue holes distributed across North Andros using a WTW LF91 conductivity/temperature probe, and values compared with those of bank and open ocean waters. In addition RCM records provided evidence of temporal variation in salinity and temperature of saline discharges from oceanic blue holes on the east coast of Andros.

Results

Magnitude of saline ground water circulation.

The discharge and head recorded at South Mastic oceanic blue hole for a representative 48 hour period are shown in Figure 2. While the semi-diurnal response to local tidal head can clearly be seen, the duration of the outflow phase is significantly longer than that of the inflow phase. Furthermore, outflow velocities are consistently higher and less variable than those of the inflow which are strongly influenced by local semi-diurnal tidal asymmetries. Clearly there is a net discharge of saline ground water at this site, which averaged 2.0×10^5 m^3 per tidal cycle during the 17 day record. A much longer record is available from the smaller Rat Cay oceanic blue hole, where over the 29 week period of observation an average of 1.7×10^4 m^3 of saline ground water was discharged per tidal cycle. This is significantly less than the discharge measured at South Mastic blue hole, but never-the-less equivalent to a cumulative discharge of 6.8×10^6 m^3 over the observation period. This average conceals a significant seasonal variation, with a relatively small net discharge during the summer, increasing significantly into the autumn and winter, suggesting temporal variation in the magnitude of the force(s) driving circulation.

Ten comparable oceanic blue holes are known to discharge saline ground waters on the east coast of North Andros. If we assume that the monitored discharges from Rat Cay and South Mastic blue holes are representative of long-term average discharges, lower and upper estimates of the total discharge of 3.3×10^5 and 4.0×10^6 m^3/d can be derived. This is equivalent to a net outflow of 4.1 to 49 $m^3/d/m$ distributed along the 80 km length of the east coast of North Andros. However, total ground water discharge may be greater as other small conduits may be present and unobserved discharge may also occur from the bank margin directly into the Tongue of the Ocean. Assuming an effective aquifer thickness of 142 m (with flow constrained below the base of the fresh-salt water mixing zone at -26 m but above -168 m where the average density of blue hole waters equals that in the adjacent ocean), the rate of saline ground water flow can be estimated as 2.9 to 35×10^{-2} m/d.

The distribution of salinity and temperature within the saline ground water body provides a direct indication of ground water source and evolution, and thus the mechanism(s) driving circulation. Salinity data is summarised in Figure 3A. Ocean waters in the Straits of Florida and the Tongue of the Ocean are of comparable salinity (mean salinity 36.3 and 36.6 ‰ respectively), the latter being slightly more saline due to it's enclosed position (Busby and Dick, 1964). In comparison, ground waters discharging from oceanic blue holes on the east coast of North Andros during July/August have a terminal blow salinity of 37.70 ± 1.65 ‰ at the end of the discharge phase. These elevated salinity waters can only be derived from the

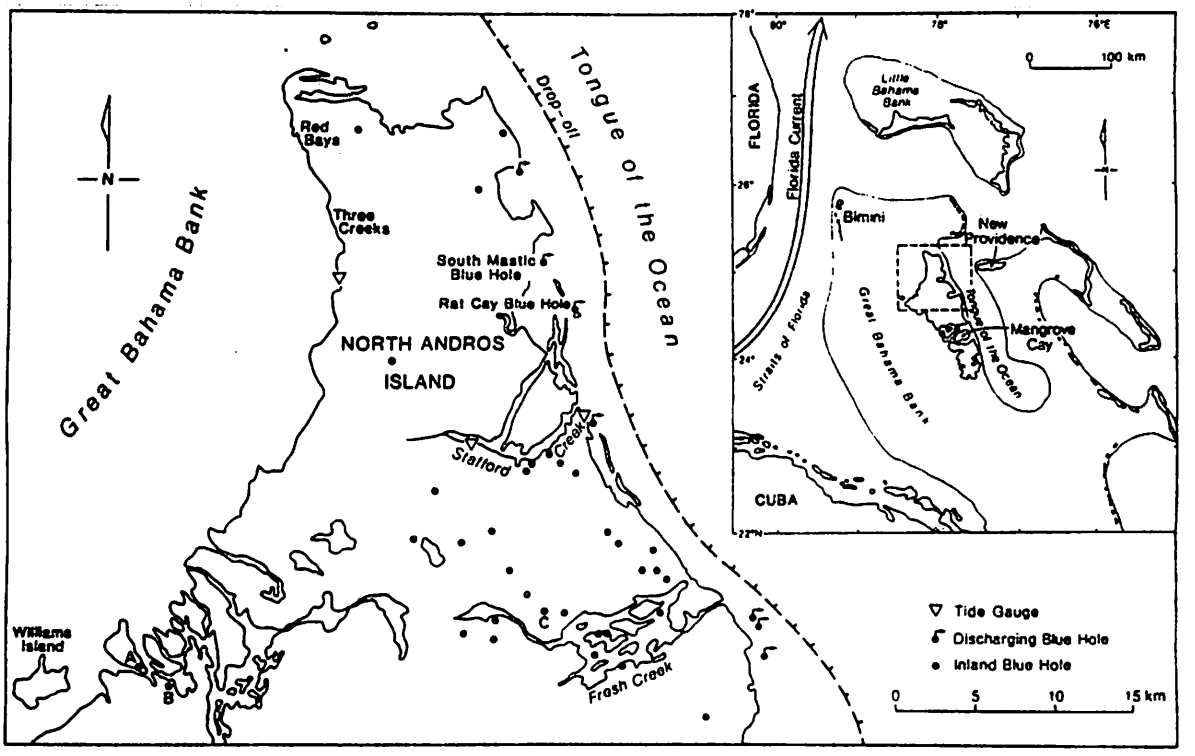

Figure 1 North Andros study area showing inland and oceanic blue holes used for sampling.

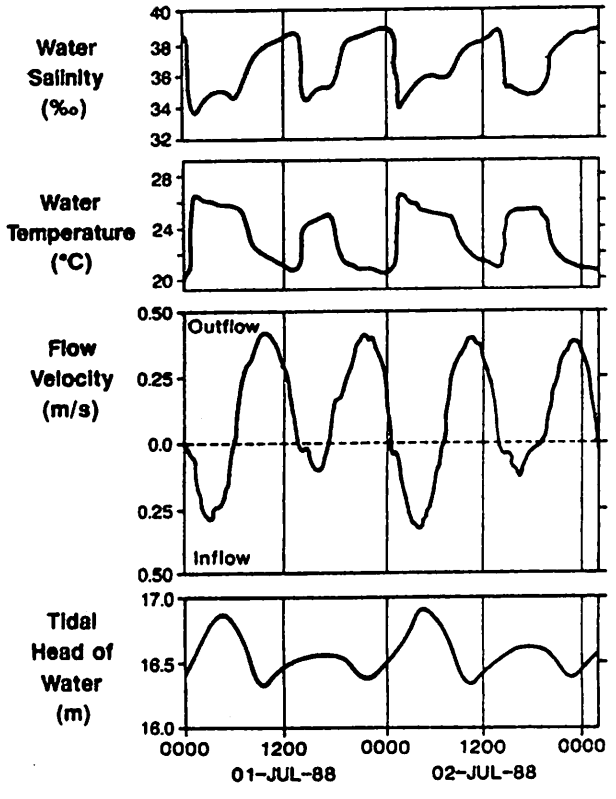

Figure 2 Representative section of recording current meter record from South Mastic Blue Hole for a 48 hour period in July 1988, showing variation in local tidal head, velocity and direction of flow, water salinity and temperature. (Whitaker and Smart, 1990).

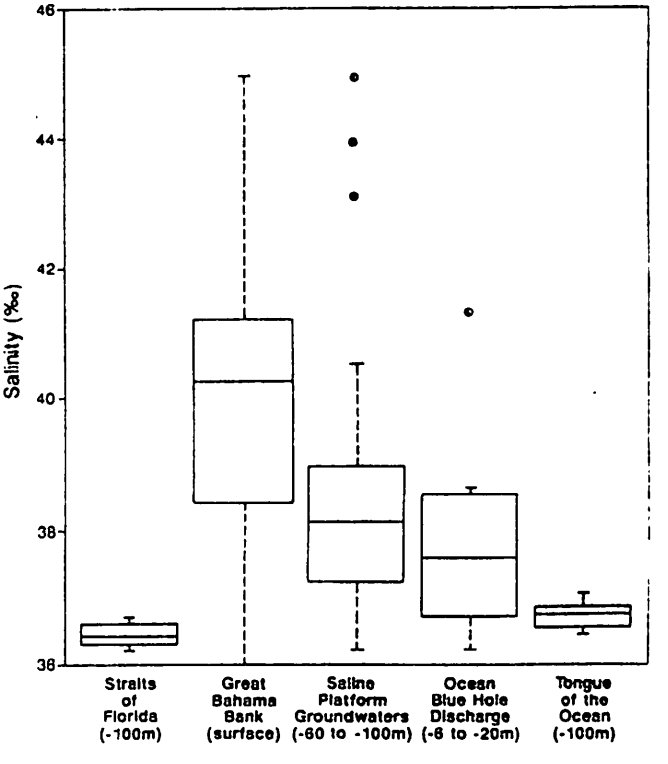

Figure 3 Boxplot of salinity of open and bank sea waters and platform groundwaters sampled in inland blue holes, showing median, upper and lower quartiles, and range. Statistical outlines are marked by black circles and for inland blue holes comprise the west coast sites. (Whitaker and Smart, 1990).

Great Bahama Bank to the west of North Andros Island. Here seasonally high evaporation rates and restricted circulation elevate the salinity to more than 38 ‰ over large areas of the bank, while in the immediate lee of the island salinities may exceed 45 ‰ (Cloud, 1962; Simms, 1984). Elevated salinity waters (37.20 ± 1.85 ‰) are also present beneath the fresh-salt water mixing zone in inland cenote blue holes on North Andros, while two blue holes on the west coast are significantly more saline (44.45 ± 0.70 ‰), comparable with the most saline bank waters. Additionally, oceanographic studies of the Tongue of the Ocean (Busby and Dick, 1964) have recognised a plume of water of slightly elevated salinity (up to 37.0 ‰) at depths of 160-180 m adjacent to the eastern side of Andros Island.

Within the oceans surrounding the platform temperatures decrease with depth at an average rate of 1.7°C/100 m in the mixed surface layer inceasing to approximately 5.5°C/100 m below this in the thermocline layer (Figure 4A). In contrast, for static ground waters temperature would be expected to increase with depth due to geothermal heating, at a rate comparable to that in adjacent Peninsula Florida (2.5°C/100 m; Kohout *et al.*, 1977). On Andros, ground water temperatures in individual inland blue holes are virtually isothermal below the depth of surface warming due to in-hole convection, with an average temperature of 24.4 ± 0.5°C. However the ground water temperature appears to be controlled by the maximum depth of the blue hole, with the mean temperature of the isothermal section decreasing with depth at a rate of 1.4°C/100 m. There is also a strong inverse relationship between ground water temperature distance from west to east across the island (Figure 4B), with cooling at an average rate of 1°C/45 km from the east coast. Furthermore, elevated salinity waters discharging from oceanic blue holes are significantly colder than both surface sea waters (annual range 22-33°C) and mean annual temperature (25°C), with a minimum temperature of 21°C during the summer.

Discussion

Models of saline ground water flow through the Great Bahama Bank.

Volumetric measurements of ground water discharge from oceanic blue holes on the east coast of Andros indicate that large-scale circulation of saline ground water occurs within the Great Bahama Bank. Both these discharges and ground waters at depth beneath the island are of elevated salinity and must thus derive, at least in part from the shallow banks on the opposite side of the island and flow eastwards beneath Andros to discharge into the Tongue of the Ocean. This circulation is probably driven by reflux of waters of only slightly elevated salinity, as predicted by Simms (1984). Such reflux would be at a minimum during the rainy late summer and early autumn but increase over the subsequent dry season as a result of evaporation, a pattern observed in the Rat Cay discharge record. The spatial distribution of salinities suggests that reflux waters flowing eastwards mix and become diluted with normal salinity water. Refluxing bank waters enter the platform at or slightly below (in the case of winter dominant flux) the mean annual temperature but would be expected to be warmed by the flux of geothermal heat as they pass through the platform. This is at variance with observed saline ground water temperatures that are significantly colder than mean annual temperature and decrease both with depth and with distance from west to east. The similarity between ground water and oceanic temperature profiles indicates the operation of a second circulation system involving cold normal salinity sea water which conservative mixing calculations suggest is derived from depths in excess of 260 m (Whitaker *et al.*, in press).

This cold circulation system may be driven by geothermal convection (Figure 5A) as documented for Florida by Kohout *et al.* (1977). Alternately, the temperature distribution observed in inland blue holes may be better explained by a net flow of sea water eastwards from the Straits of Florida beneath Andros Island (Figure 5B). Such a circulation could be driven by a sustained difference in sea-surface elevation across the platform associated with atmospheric or oceanic circulation. Where the Gulf Stream is restricted and turns northwards in the Straits of Florida, an average head difference of 66 cm is generated between Miami and Bimini (Maul, 1986). If such a difference were to be maintained across the northwest Great Bahama Bank it would be sufficient to drive net eastward movement of ground water due to the high cavernous permeability.

AQUEOUS GEOCHEMISTRY

Methods

Saline ground waters were sampled from oceanic blue hole discharges at the termination of the outflow phase (n=9) and from inland blue holes, both cenote holes distributed across North Andros (n=17) and sites developed on extensional fractures paralleling

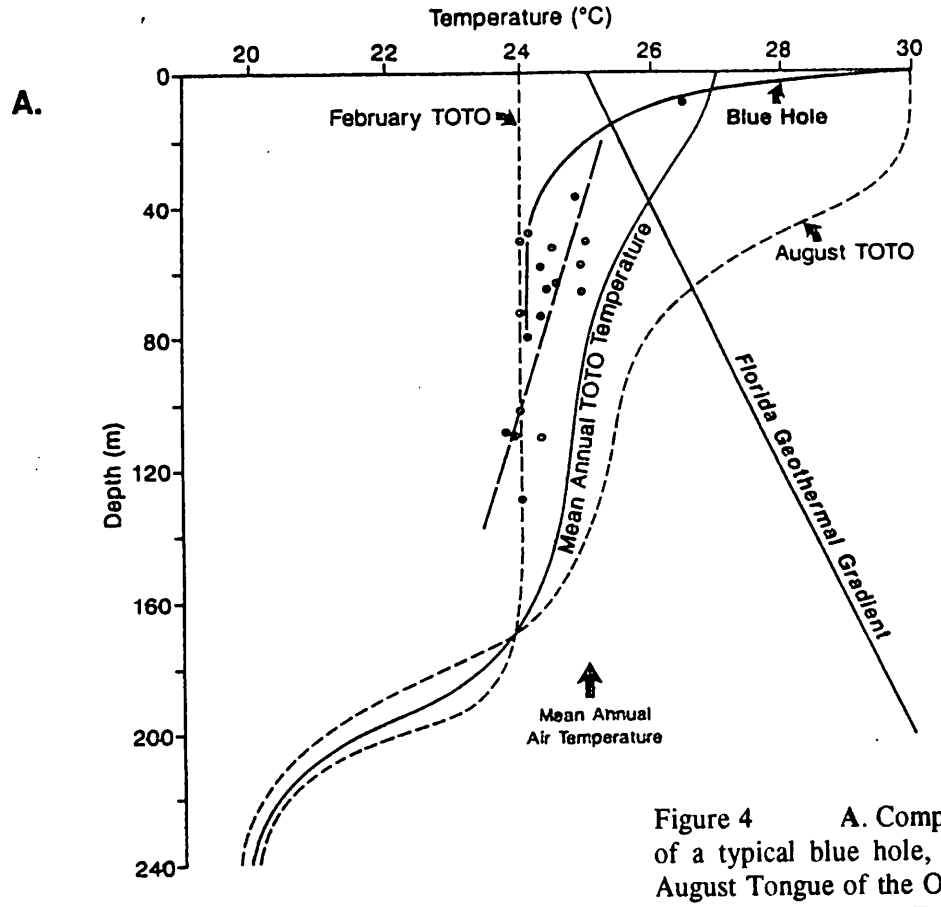

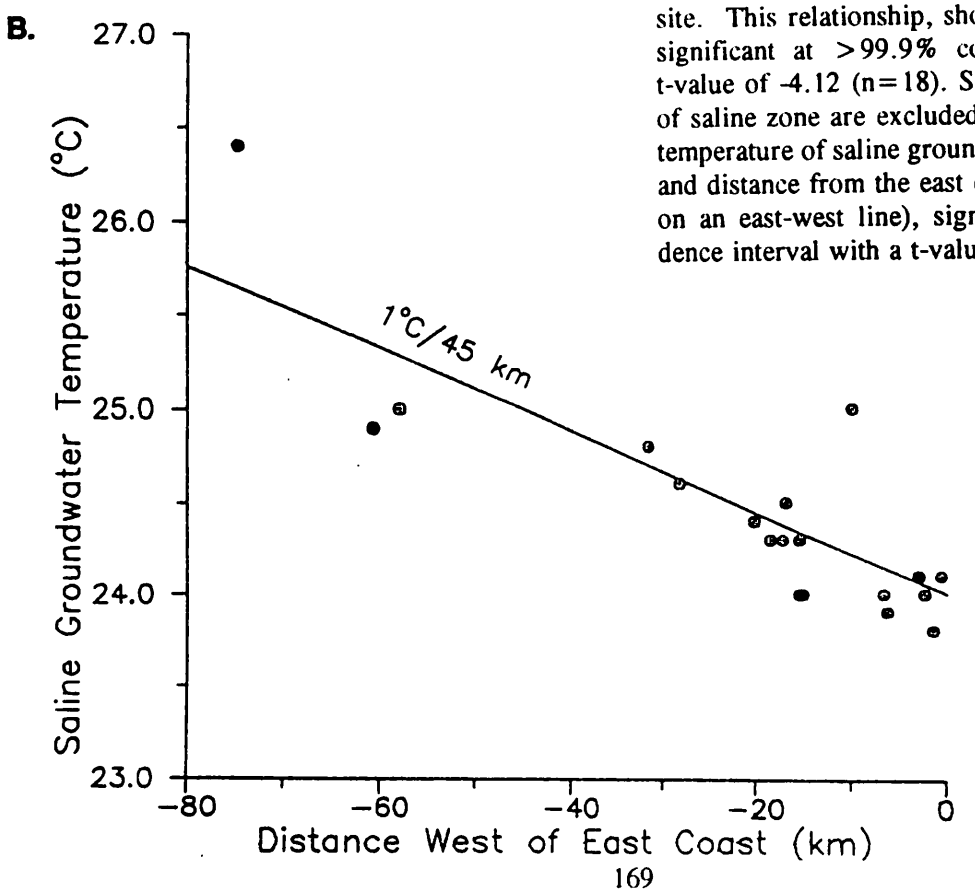

Figure 4 **A.** Comparison of temperature profiles of a typical blue hole, mean annual, February and August Tongue of the Ocean profiles and the Florida geothermal gradient. For individual inland blue holes solid circles indicate the temperature of the isothermal saline groundwater body and maximum depth of the site. This relationship, shown by the dashed line, is significant at >99.9% confidence internal with a t-value of -4.12 (n=18). Sites which intersect <5 m of saline zone are excluded. **B.** Relationship between temperature of saline groundwater in inland blue holes and distance from the east coast of Andros (measured on an east-west line), significant at >99.9% confidence interval with a t-value of -5.02 (n=18).

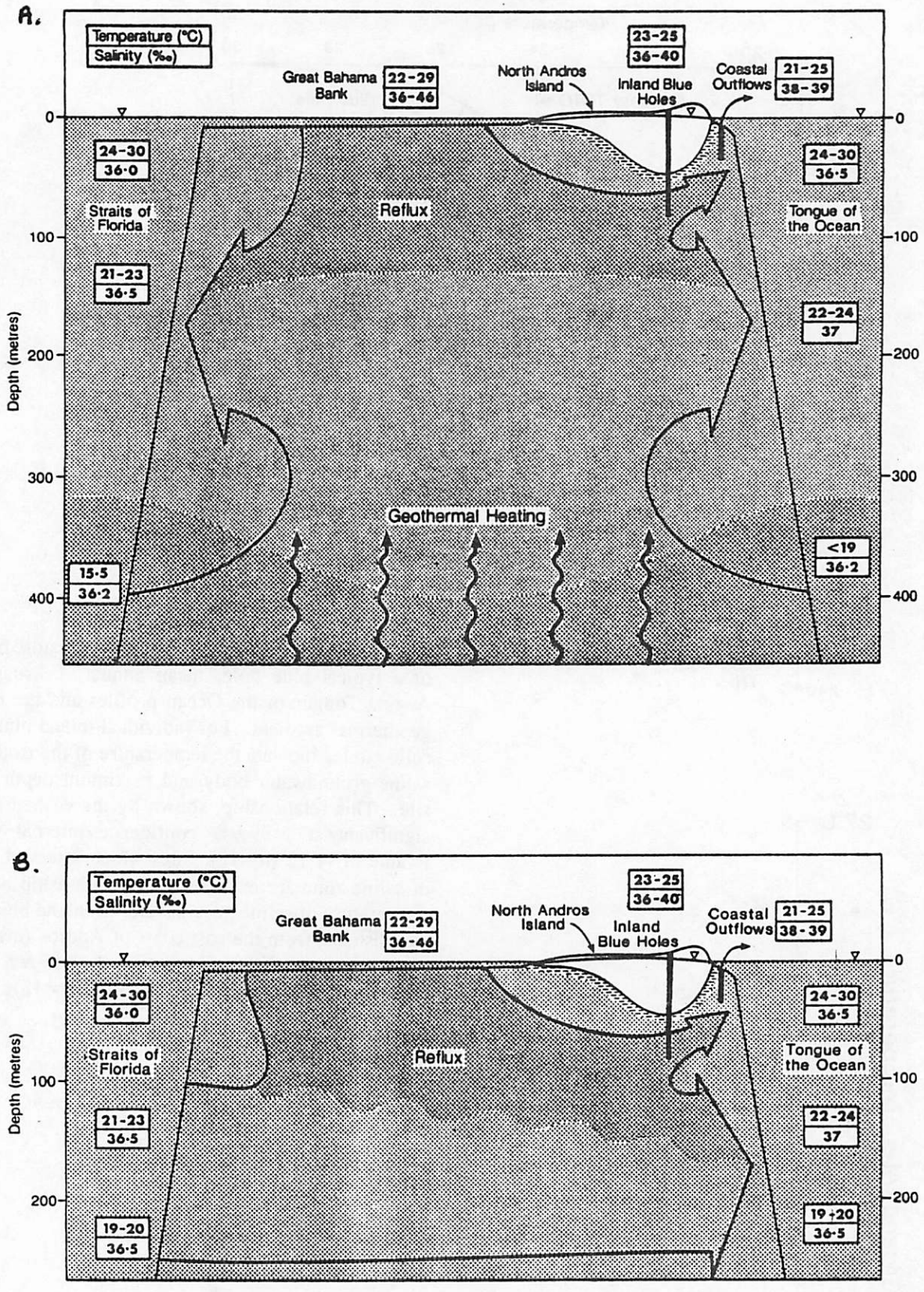

Figure 5 Two alternative saline circulation systems postulated for the northwest Great Bahama Bank. **A.** Thermal (Kohout-type) with reflux drive. **B.** Reflux with trans-bank difference in sea surface elevation. Weight of stipple is proportional to groundwater density. (Whitaker *et al.*, in press).

the eastern bank margin on South Andros (n=14) (Smart *et al.*, 1988). Samples were collected both using a Wuidart bore-hole sampler and *in situ* by divers using 1.5 L sampling tubes. At the surface samples were flowed through a closed cell in which pH (± 0.02 pH units) and dissolved oxygen (± 1% O_2 saturation) were measured. Sub-samples were taken for immediate measurement of alkalinity and calcium by titration, and for later analysis of magnesium, sodium, potassium and strontium by spectrophotometry, chloride by Mohr titration and sulphate by turbimetry. All dilutions were weighed and analytical precision was ± <1% (with the exception of sulphate ± 4.5%). In addition reduced sulphur was determined by iodometric titration (± 1.5%) and dissolved organic carbon analysed by high temperature catalytic oxidation (± 28%). Ion balance errors were all <5% with an average deviation from zero of ± 1.4%, and accuracy of magnesium and chloride analyses was confirmed by independent analysis. Saturation indicies for calcite, aragonite, ordered and disordered dolomite (K_D $10^{-16.52}$ and $10^{-18.06}$ respectively; Helgeson *et al.*, 1981) and equilibrium PCO_2 were calculated using the aqueous speciation model SOLMINEQ.88 (Kharaka *et al.*, 1988).

The nature and degree of water-rock interaction was investigated by calculating the excess amount of magnesium and calcium (Mg_{xs} and Ca_{xs}) in solution relative to the concentration predicted from conservative mixing of source waters, chloride being used as a conservative tracer. For saline ground waters end-members for mixing calculations were Tongue of the Ocean and Great Bahama Bank input waters, while oceanic discharges were modelled as a product of mixing of average saline ground waters beneath eastern Andros and local east coast bank waters. Combined 1 sigma root mean squared analytical uncertainties are ± 28 mg/L for Mg_{xs} and ± 8 mg/L for Caxs (see Whitaker, 1992 for full treatment of errors).

Results

Diagenetic potential of saline ground waters.

The potential for carbonate diagenesis is critically dependent upon the PCO_2 of the ground waters. The PCO_2 of bank and open ocean source waters is close to the atmospheric value, but within the Holocene sediments mantling the bank surface the PCO_2 of porewaters can be significantly elevated (Morse *et al.*, 1985), suggesting a PCO_2 for cenote waters of up to 0.17% (based on a porewater PCO_2 of 0.55% for fine grained pelletal muds). The PCO_2 of saline waters from inland cenotes indicates substantial CO_2 enrichment, with values of 0.34 ± 0.17% for west coast cenotes increasing to 1.04 ± 0.20% in central and eastern cenotes suggesting subsurface generation of CO_2 (Figure 6A). The PCO_2 of waters from inland fracture blue holes and east coast oceanic discharges remains elevated compared to input waters, but is significantly lower than that of cenotes, in the case of discharges some 0.4% less than the PCO_2 predicted from conservative mixing of cenote ground waters and east coast bank waters.

The observed enrichment of CO_2 is caused by *in situ* oxidation of organic matter along the saline ground water flow path. Concentrations of organic matter in the ground waters are significantly elevated (13.2 ± 3.9 mg/L DOC) compared with source waters (7.3 ± 2.7 mg/L DOC), and oxidation of organic carbon in the anoxic saline ground waters occurs by bacterially mediated sulphate reduction. Cenote ground waters contain reduced sulphur species (3.8 ± 6.3 mg/L) which are absent in input sea waters, and show some evidence of sulphate depletion (126 ± 133 mg/L); the cumulative effect of progressive sulphate reduction along the saline ground water flow path. Fracture waters, however, show no significant sulphate depletion (-14 ± 165 mg/L) while oceanic discharges are slightly enriched (+43 ± 120 mg/L) indicating re-oxidation of reduced sulphur species as previously reported for oxic fresh ground waters from inland cenotes (Bottrell *et al.*, 1991).

The elevated CO_2 concentrations resulting from this oxidation of organic matter cause a significant reduction of carbonate saturation in all saline ground waters compared to source sea waters. Cenote and fracture waters are driven to equilibrium with respect to calcite, although oceanic discharges are marginally supersaturated to both calcite and aragonite (Figure 6B). There is a similar reduction in dolomite saturation in saline ground waters compared to source waters, but all waters retain the thermodynamic potential to precipitate ordered, and in most cases disordered, dolomite (Figure 6C).

Nature of diagenesis in the saline zone.

Both cenote and fracture blue hole waters are significantly depleted in magnesium (Figure 7A) with Mg_{xs} of -52 ± 45 mg/L and -41 ± 15 mg/L respectively. The total Mg_{xs} of -36 ± 38 mg/L for oceanic discharge indicates that the saline ground water component is depleted by 15 ± 56 mg/L in addition to that observed in central and eastern cenotes. Thus saline ground waters show a total magnesium depletion

of 67 ± 72 mg/L along the complete flow path. Inland cenote and fracture blue hole waters also both show significant enrichment of calcium compared to source water predictions (Figure 7B) with Ca_{xs} of +18 ± 17 mg/L and +14 ± 27 mg/L respectively. In contrast oceanic discharges are depleted in calcium with a Ca_{xs} of -15 ± 8.5 mg/L. Although bank source waters are enriched in strontium compared with open ocean waters due to stabilisation of aragonite to calcite, the Sr_{xs} of all saline ground waters is not significantly different from zero ± 1 sigma analytical uncertainty (see Whitaker, 1992).

Waters may become depleted in magnesium as a result of either precipitation of high-magnesium calcite cements or dolomitisation. Precipitation of high-magnesium calcite would consume both magnesium and calcium in an average molar ratio of 0.12:0.88 (Garrels and Wollast, 1978). In saline ground waters from inland cenote and fracture blue holes the observed magnesium depletion is accompanied by calcium enrichment (Figure 7). In the absence of significant calcium depletion, high magnesium calcite could only form by stabilization of aragonite which would result in waters becoming enriched in strontium. However strontium concentrations in saline ground waters are within analytical uncertainty of those predicted by conservative mixng of input waters, excluding the possibility of high-magnesium calcite precipitation. This suggests that dolomitisation is occuring, accompanied by calcite dissolution, in accordance with observed dolomite and calcite saturation indicies. While oceanic discharges are depleted in both magnesium and calcium, the molar Ca_{xs}:Mg_{xs} ratio together with their hydrological position downstream of the inland blue holes suggests dolomitisation along the flow path followed by precipitation of high- or low-magnesium calcite cements. Cementation thus appears to be restricted to the platform margin and may be associated with the local, tidally-driven pumping of sea water observed in the RCM records from oceanic blue holes (Figure 2).

The nature of the dolomitisation reaction is indicated by the molar Ca_{xs}:Mg_{xs} ratio of the ground waters. Dolomitisation is unlikely to occur *via* primary precipitation (Reaction 1, Table 1) which would consume both calcium and magnesium. It may however occur by replacement, either releasing calcium (Reaction 2A, Table 1) or consuming carbonate (Reaction 2B, Table 1). For inland cenote and fracture blue hole waters, the molar magnesium depletion is an average of 4.3 and 3.6 times larger than the calcium release, suggesting dolomitisation occurs predominantly (*c.* 75%) by replacement with consumption of carbonate.

Discussion

Rate of dolomitization by saline ground waters.

The rate of dolomitization can be calculated from the product of the estimated rate of ground water flow and the observed magnesium depletion. A magnesium depletion of 67 mg/L, the cumulative depletion of saline ground waters from inland and oceanic blue holes, is equivalent to precipitation of 0.51 g dolomite per litre of discharging ground water. This dolomite is assumed to be evenly distributed along the length of the ground water flow path, taken to be 100 km from the centre of the flooded Great Bahama Bank to the eastern platform margin. By using a specific gravity of dolomite of 2.85 g/cm^3, and the flow rate of 2.9 to 35 x 10^{-2} m/d, the rate of dolomitisation of 1.8 to 22 x 10^{-6}%/a can be calculated.

Thermodynamic and kinetic drives to dolomitisation.

The geochemistry of saline ground waters beneath Andros Island indicates that dolomitisation is occuring by replacement of calcite. These waters are supersaturated with respect to dolomite and thus have the thermodynamic potential for dolomitization. While the degree of supersaturation is significantly less than that of open ocean and bank source waters, it may be

1 Primary Precipitation

$$Ca^{2+} + Mg^{2+} + 2CO_3^{2-} \text{ -------> } CaMg(CO_3)_2$$

2. Replacement Dolomitisation

A. $$2CaCO_3 + Mg^{2+} \text{ -------> } CaMg(CO_3)_2 + Ca^{2+}$$

B. $$CaCO_3 + Mg^{2+} + CO_3^{2-} \text{ -------> } CaMg(CO_3)_2$$

Table 1 Principal dolomitisation reactions.

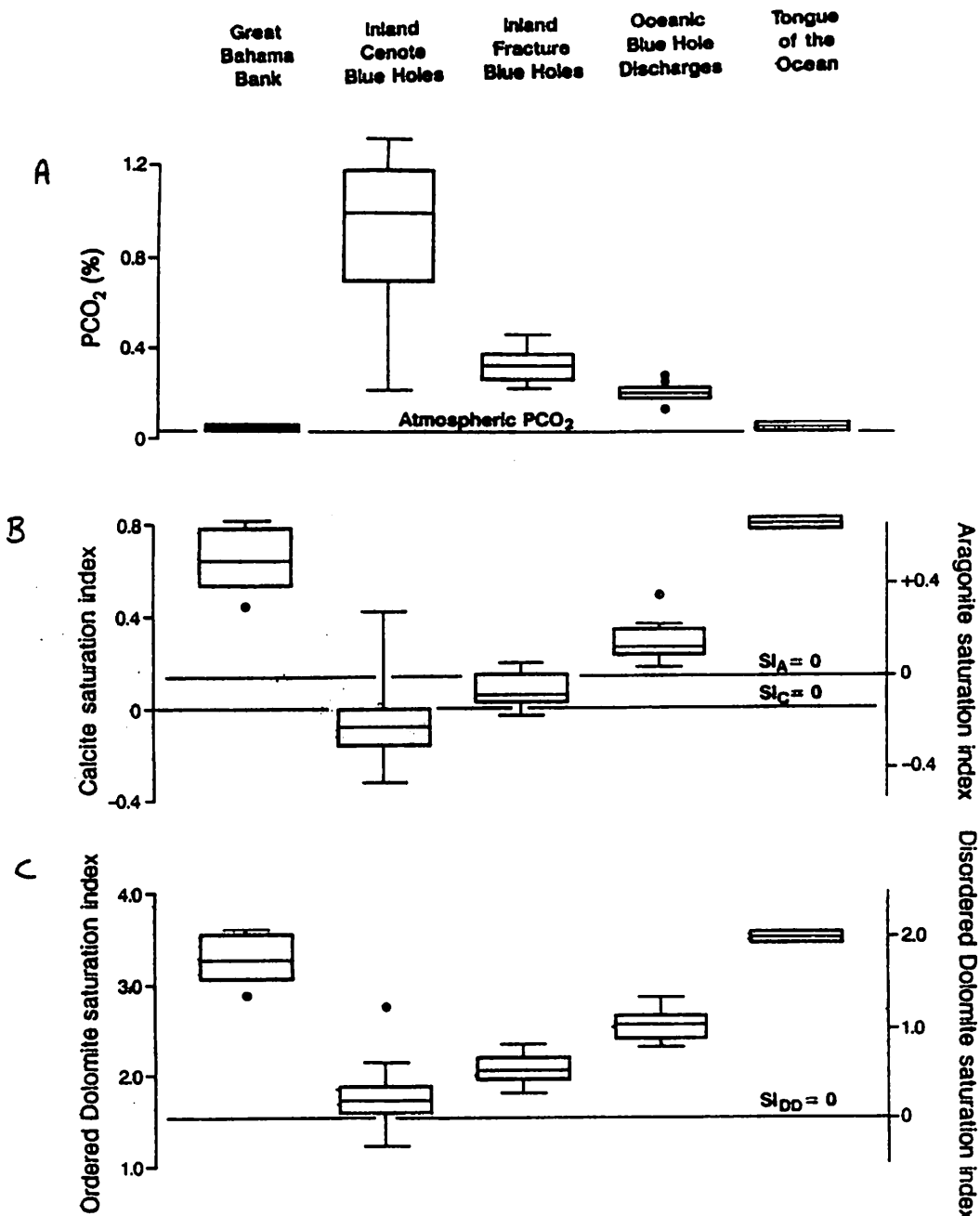

Figure 6 Boxplots of **A.** PCO_2, **B.** calcite and aragonite saturation and **C.** ordered and disordered dolomite saturation for inland cenote and fracture blue holes and oceanic discharges compared with input bank and open ocean waters.

sufficient to drive dolomitisation where there is active ground water circulation through the platform. Indeed, the reduced degree of saturation observed in the ground waters may be critical in driving dolomitisation under conditions of calcite undersaturation and dolomite supersaturation, as proposed for the fresh-salt water mixing zone by Badiozamani (1973), and/or by aiding segregation of magnesium and calcium in the dolomite crystal (Gaines, 1980). Alternatively, dolomitisation may be enabled by supression of the kinetic controls which appear to inhibit dolomitisation by sea water at near surface temperatures and pressures (Lippmann, 1973). There is a positive linear relationship between magnesium depletion and sulphate depletion ($t = 3.39$, $p = 99.8\%$, $n = 38$) despite the large combined analytical uncertainty for SO_{4XS} and re-oxidation of reduced sulphur species in oceanic discharges. However observed sulphate depletions are relatively small compared to those reported to enhance dolomitisation in laboratory experiments (Baker and Kastner, 1981), and thus this relationship is more likely due to autocorrelation rather than direct causality. Sulphate depletion is controlled by the supply of organic matter which may have a direct effect on dolomitisation either by catalysis (Morrow, 1982) or by differential complexing by organic acids which reduces the effective Ca: Mg ratio (Harrison and Thyne, in press). However these effects are poorly understood and absolute concentrations of organic catalysts and complexing acids are relatively low.

Laboratory studies have demonstrated a clear association between dolomitisation and increased

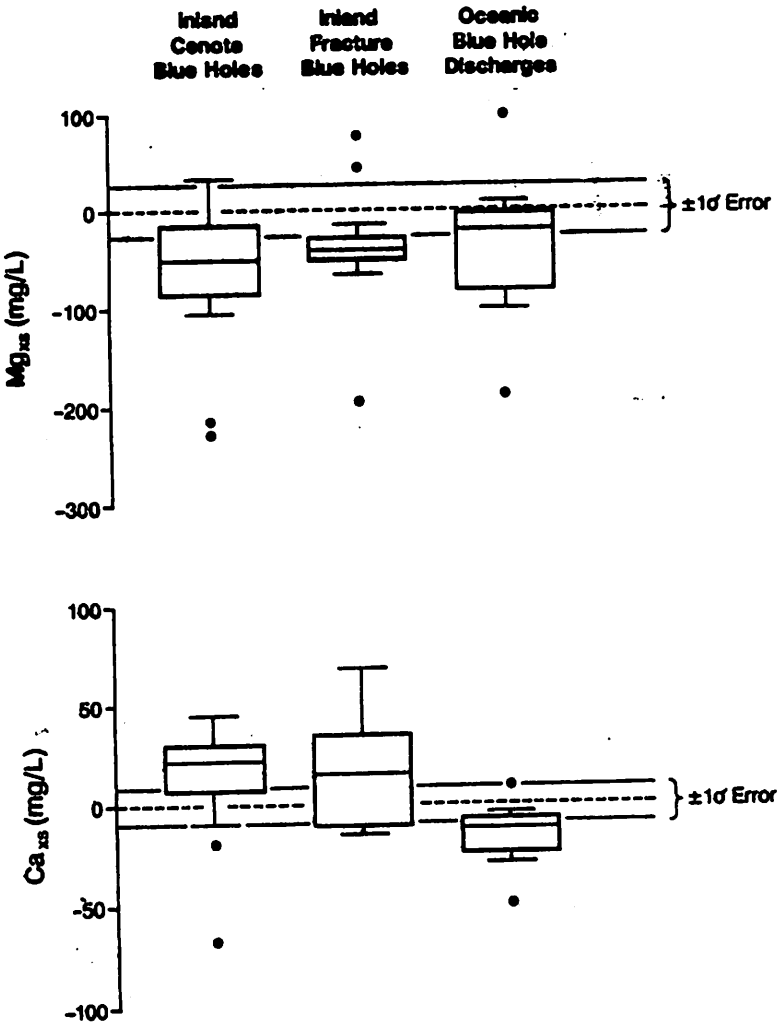

Figure 7 Boxplots of A Mg_{xs} and B Ca_{xs} for inland cenote and fracture blue holes and oceanic discharges. (Whitaker *et al.*, *in press*).

alkalinity, here derived from bacterial oxidation of organic matter. The differential in Gibbs free energy of reaction for the replacement dolomitisation reactions (-1.83 kilocal/mole for Reaction 2A compared with -13.24 for Reaction 2B) demonstrates the important role of additional carbonate which facilitates carbonate ion penetration of the hydrated magnesium ion barrier on the crystal surface (Lippmann, 1973). There is a strong positive linear relationship between PCO_2 and SIC for inland cenote waters ($t=5.52$, $p>99.9\%$, $n=13$ excluding 2 outliers). This is the inverse of the normal negative logarithmic pattern resulting from degassing and/or calcite dissolution which is evident for inland fracture waters and oceanic discharges, and can only be explained by calcium release due to dolomitisation under conditions of high carbonate activity. Thus, while autocorrelation prevents definition of the precise nature of any kinetic controls on dolomitisation, organically-mediated reactions, most importantly the resulting increase in carbonate activity, appear to be of importance.

SHALLOW DOLOMITES FROM SOUTH ANDROS

Methods

A vertical suite of wall-rock samples was collected from Stargate fracture blue hole, South Andros, over the depth range 0-43 m, in order to examine the distribution and nature of any Pleistocene dolomites within the platform. Thin-sections were stained with Alazarin Red S and examined using a petrographic microscope. The stochiometry of the dolomites was calculated from calcium and magnesium concentrations from electron microprobe analyses. Two methods were used to examine the stable isotope geochemistry of the dolomite; standard mass-spectrometric analysis of CO_2 gas from a dolomite concentrate, and spot analyses on thin sections using a laser ablation system (LASSIE, Smalley *et al.*, 1992). A scanning proton microprobe (SPM) was used to determine the major trace element content of the dolomite (Frasar, 1990), and maps and point analyses were carried out on dolomite grains using proton-induced x-ray analysis (PIXE). The timing of dolomitisation was estimated using strontium isotope analysis of dolomite concentrate prepared by dissolution of all calcite from a bulk sample in acetic acid.

Results

Distribution and petrography of shallow dolomites.

While dolomite is absent in samples from the brackish fresh-water lens (0-14 m depth) and the fresh-salt water mixing zone (14-28 m depth), minor amounts were found in samples from the zone of saline ground water below a depth of 29 m to a maximum sampled depth of 43 m. Within this zone dolomite abundance increases with depth apparently due to relatively recent dissolution in the upper part of this zone, probably associated with the organic rich base of the mixing zone (Whitaker, 1992).

The host rock consists of coral and skeletal

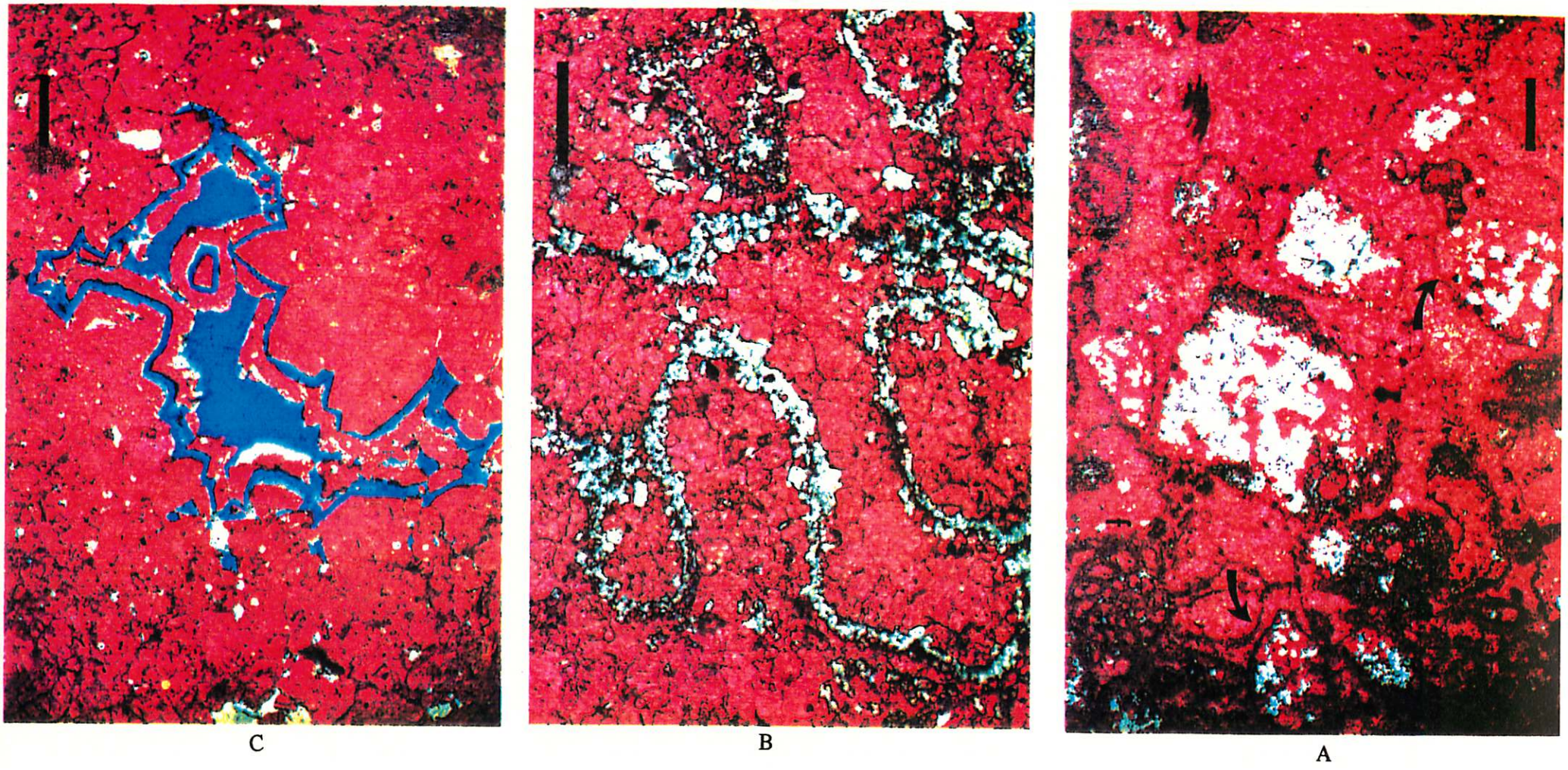

Figure 8 Thin section photomicrographs from Stargate wall rock samples. Calcite has been stained red with Alazarin Red S and pore space is impregnated with blue plastic resin. **A.** Dolomite patches and isolated small rhombs in a well cemented low-Magnesium calcite grainstone. Note micritic rinds outlining former grains (arrows) and small foraminifera (F). Scale bar - 200 μm, sample depth 31.5 m. **B.** Dolomite cement (?) on a micritic rind tracing the outline of a scleractinian coral. Scale bar = 100 μm, sample depth 31.5 m. **C.** Outline of a former (dolomite?) rim cement. Scale bar = 200 μm, sample depth 29 m. (Whitaker *et al.*, in press).

grains, and both matrix and cement are stabilized low-magnesium calcite. Dolomite is found both as a matrix replacement and primary cement, with a patchy distribution, and typically comprises 1-2%, but in places up to 5%, of the rock. Four dolomite fabrics can be recognised; isolated euhedral rhombs, 4-5 μm diameter (Figure 8A); patches of anhedral crystals, commonly 30-50 μm but up to 200 μm diameter (Figure 8A); fabric selective replacement of allochems (Figure 8B); and minor rim cements (Figure 8C). The dolomite is thus petrographically distinct from many mature ancient dolomites, but resembles many recent immature dolomites described from the Carribean (Ward and Halley, 1985; Humphrey, 1988; Vahrenkamp and Swart, in press).

Geochemistry and isotopic characteristics of shallow dolomites.

Dolomites are non stoichiometric, (44.4 $\pm$ 0.8 mole % $MgCO_3$) and are relatively strontium-poor (152 $\pm$ 34 %o) compared to other supposedly marine dolomites (for example Behrens and Land, 1972). However, molar cation ratios predicted for fluids in equilibrium with the dolomites (calculated by the method of Wogelius *et al.*, 1992) are consistent with precipitation from sea water or a slightly reduced pore-fluid derived from sea water. The limited range of iron (148 $\pm$ 35 ppm) and manganese (15 $\pm$ 3.5 ppm) concentrations indicates the maintenance of relatively constant slightly reducing the conditions. Linescans and maps show no obvious trace element zoning.

Carbon and oxygen stable isotope determinations on coexisting calcite and dolomite from a sample at -35 m are shown in Figure 9. A mixing trend is evident in isotopic signatures between matrix calcite and the dolomite concentrate, suggesting that the large LASSIE spot size (50-70 μm) necessitated by the high transparency of the thin-section may have caused partial admixture of CO_2 gas from the matrix calcite. The Stargate dolomites thus have an isotopic signature of approximately +3.5%o $\delta^{18}O$ and +2.5%o $\delta^{13}C$, essentially the same as that of older massive dolomites found elsewhere in the Bahamas (Vahrenkamp and Swart, in press) and consistent with precipitation from sea water (1%o SMOW) at 20-22 °C. This is slightly colder than modern saline ground water temperatures in Stargate (24-25 °C) but comparable with minimum values for oceanic blue hole discharges.

The strontium isotope ratio of 0.709137 for dolomite from the -35 m deep sample corresponds to a sea water strontium isotope age of 0.4-0.8 Ma. This is the oldest possible age of dolomitisation and the dolomites may be younger if strontium with an older isotopic signature has been incorporated. The age of the host limestones is estimated by correlation with core U-1 on North Andros where magnetostratigraphy and biostratigraphic marker horizons indicate an age of 1.5-2.5 Ma for rocks at 30-40 m depth (McNeil, 1989). Thus the shallow Stargate dolomite is significantly younger than the host limestone and is also younger than the massive Pio-Pleistocene dolomites found at depth (>53m in core U-1) which are common throughout the Bahamas (Vahrenkamp *et al.*, 1991).

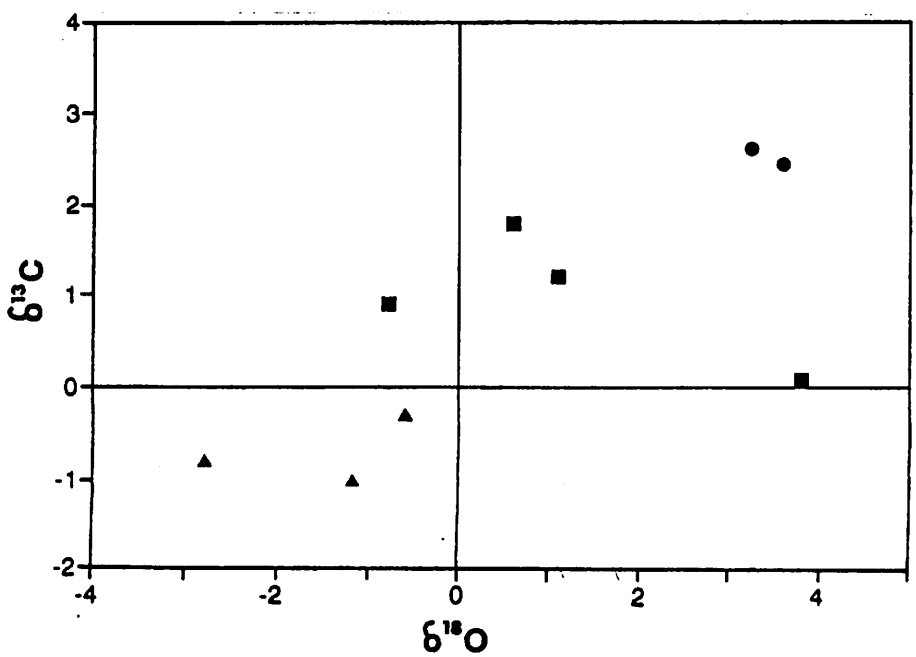

Figure 9 Cross plot of carbon and oxygen stable isotopes of -38 m Stargate wall rock sample. Calcites and dolomites measured with LASSIE are triangles and squares respectively, and concentrated dolomite from a bulk sample are circles. Mixing between calcite and dolomite end-members is indicated. (Whitaker *et al.*, in press).

Discussion

Can the modern saline ground

water circulation account for the shallow Stargate dolomites?

The sparse Pleistocene dolomites observed in wallrock samples from Stargate are petrographically typical of many 'recent' dolomites. Geochemically they are compatible with formation from waters of near-normal sea water salinity at temperatures a few degrees less than mean annual temperature and under slightly reducing conditions. Such a parent fluid is thus very similar to the saline ground waters currently circulating through the platform, and which are magnesium depleted. The Stargate dolomites clearly postdate the host sediments, but 2 models of the strontium isotope age of 0.4-0.8 Ma are possible. Dolomitisation could have occured slowly over an extended period after deposition whenever favourable conditions existed, and thus the age represents a bulked average for this period. Alternatively, dolomitisation occured in a single phase of limited duration, as has been proposed for older Bahamian dolomites (Vahrenkamp *et al.*, 1991). The absence of trace element zoning in proton probe maps suggests a single growth phase, although zoning would not be expected if aqueous geochemical conditions were similar during multiple phases of growth. Thus evidence regarding the 'age' of the dolomite remains equivocal.

Calculations combining hydrological and aqueous geochemical data suggest a present day rate of dolomitisation by saline ground waters of 1.8 to 22 x 10^{-6}%/a. The large range of this estimate reflects considerable uncertainties, particularly in the magnitude of the saline ground water circulation. Considering carbonates from a depth of 30 m in Stargate and assuming an average subsidence rate of 20 m/Ma (McNeil, 1989), the maximum period for dolomitisation would be 1.5 Ma. However this ignores periods of low sea-level when these rocks would be resident within the vadose zone, freshwater lens or mixing zone. Furthermore, saline circulation systems, such as developed at present, depend upon shallow flooding and development of restricted seawater circulation on the bank. Given Pleistocene sea-level fluctuations, such conditions could have occurred for approximately 10% of the time, giving a total period of dolomitisation of approximately 150 ka. Thus 0.27 - 3.3% dolomite could be generated in rocks currently at -30 m by circulation of saline ground water. In thin section, samples from Stargate typically contain 1-2% dolomite (locally up to 5%), within the range of order of magnitude estimates derived from present day rates of dolomitisation.

CONCLUSIONS

1. Large-scale circulation of saline ground water occurs through the Great Bahama Bank, with estimated flow rates in the range 2.9 to 35 x 10^{-2} m/d.
2. Slightly elevated salinity waters from the bank surface circulate through the platform and mix with cold normal salinity seawater derived from depth within the adjacent oceans.
3. The circulation of bank derived waters is probably driven by reflux as predicted by Simms (1984), while the larger-scale seawater circulation may result either from geothermal convection or from trans-bank/island differences in sea surface elevation possibly generated by the Florida Current.
4. Saline ground waters are depleted in magnesium due to dolomitisation which appears to be progressive along the flow path and occurs at an estimated rate of 1.8 to 22 x 10^{-6} %/a.
5. Dolomitisation occurs by replacement of precursor calcite with the addition of externally derived carbonate, and not by primary precipitation.
6. Saline ground waters have the thermodynamic potential for dolomitisation and are also undersaturated with respect to calcite, although kinetic factors related to organically-mediated reactions also appear to be important, particularly an elevated carbonate activity.
7. Sparse dolomites were observed in wall-rock samples from Stargate Blue Hole, South Andros at shallow depth (29-43 m) within the zone of saline ground waters.
8. These dolomites are non-stoichiometric, and geochemical and isotopic evidence indicates they formed from cool waters of near seawater salinity under slightly reducing conditions, similar to the present saline ground waters.
9. Evidence of the 'age' and rate of dolomite growth is equivocal, but abundances are compatable with those predicted from the present circulation system operating during high sea-stands since deposition.

ACKNOWLEDGEMENTS

Financial support was provided by Koninklijke/Shell Exploratie en Productie Laboratorium, Shell Bahamas, Amoco UK Exploration Company, and the Royal Society. The Insitute of Oceanographic Sciences of the Natural Environment Research Council and Environmental Sciences Division of Wimpol kindly provided, decoded and calibrated the recording current meters. Invaluable field assistance

was provided by Steve Hobbs and Rob Palmer, while Neil Sealey and Sue and Jim Phillips provided logistic support. Volker Vahrenkamp (KSEPL) assisted with petrographic examination of thin-sections, Hugh Nicholson (PB Research) undertook LASSIE analyses, Roy Wogelius (Oxford University) performed PIXE and EMA analyses, Peter Swart (University of Miami) provided stable isotope analyses of the dolomite concentrate, and Joaquin Ruiz (University of Arizona) assisted with strontium isotope analyses. Finally Simon Godden drew the diagrams and Liz Owen undertook the preparation of the manuscript.

REFERENCES

Badiozamani, K., 1973, The dorag dolomitisation model; application to the Middle Ordovician of Wisconsin: Journal of Sedimentary Petrology, v. 43, p. 965-984.

Baker, P.A. and Kastner, M., 1981, Constraints on the formation of dolomite: Science, v. 213, p. 214-216.

Behrens, E.W. and Land, L.S., 1972, Subtidal Holocene dolomite, Baffin Bay Texas: Journal of Sedimentary Petrology, v. 42, p. 155-161.

Bottrell, S., Smart, P.L., Whitaker, F.F. and Raiswell, R., 1991, Geochemistry and isotope systematics in the mixing zone of Bahamian blue holes: Applied Geochemistry, v. 6, p. 97-103.

Busby, R.F. and Dick, G.F., 1964, Oceanography of the Eastern Great Bahama Bank, Part 1. Temperature-salinity distributions: U.S. Naval Oceanographic Office, 42 p.

Cloud, R.E., 1962, Environments of carbonate deposition west of Andros Island, Bahamas: United States Geological Survey Professional Paper No. 350, 138 p.

Dawans, J.M. and Swart, P.K., 1988, Textural and geochemical alterations in Bahamian Pleistocene dolomites: Sedimentology, v. 35, p. 385-403.

Fraser, D.G., 1990, Applications of the high resolution scanning proton microprobe in the Earth sciences; an overview: Chemical Geology, v. 83, p. 27-37.

Gaines, A.M., 1980, Dolomitisation kinetics; some recent experimental studies: Society of Economic Paleontologists and Mineralogists Special Publication No. 28, p. 81-86.

Garrels, R.M. and Wollast, R., 1978, Discussion of equilibrium criteria for 2-component solids reacting with fixed composition in an aqueous phase-example, the magnesium calcites: American Journal of Science, v. 278, p. 1469-1474.

Harrison, W.J. and Thyne, G.D., *in* press, Prediction of diagenesis reactions in the presence of organic acids: Geochemica Cosmochimica Acta.

Helgeson, H.C., Kikham, D.H. and Flowers, G.C., 1981, Theoretical prediction of the thermodynamic behaviour of aqueous electrolytes at high temperatures and pressures: IV calculation of activity coefficients, osmotic coefficients and apparent molal properties at 600°C and 5 kb: American Journal of Science, v. 281, p. 1249-1516.

Humphrey, J.D., 1988, Late Pleistocene mixing zone dolomitisation, West Indies: Sedimentology, v. 35, p. 327-348.

Kharaka, Y.K., Gunter, W.D., Aggarwal, P.K., Perkins, E.H. and DeBraal, J.D., 1988, SOLMINEQ.88: A computer program for geochemical modelling of rock-water interactions: United States Geological Survey Water Resources Investigation Report No. 84-4227, 419 p.

Kohout, F.A., Henry, H.R. and Banks, J.E., 1977, Hydrogeology related to the geothermal conditions of the Floridan Plateau: in Smith, D.I. and Griffin, G.M., eds, The Geothermal Nature of the Floridan Plateau, State of Florida Bureau of Geology Special Publication No. 21, p. 1-40.

Land, L.S., 1985, The origin of massive dolomite: Journal of Geological Education, v. 33. p. 112-125.

Maul, G.A., 1986, Linear correlations between Florida Current volume transport and surface speed with Miami sea-level and weather during 1964-1970: Royal Astronomical Society Geophysical Journal, v. 87, p. 55-66.

Machel, H.G. and Mountjoy, E.W., 1986, Chemistry and environments of dolomitisation; a reappraisal: Earth Science Reviews, v. 23, p. 175-222.

McNeil, D.F., 1989, Magnetostratigraphic dating and magnetization of Cenozoic platform carbonates from the Bahamas: PhD Dissertation, RSMAS, University of Miami, Coral Gables, 210 p.

Morrow, D.W., 1982, Diagenesis 1; Dolomite - Part 1 The chemistry of dolomite precipitation: Geoscience Canada, v. 9, p. 5-13.

Morse, J.W., Zullig, J.J., Bernstein, L.D., Millero, F.J., Milne, P. Mucci., F.J. and Choppin, G.R., 1985, Chemistry of calcium carbonate rich shallow water carbonate sediments in the Bahamas: American Journal of Science, v. 285, p. 147-185.

Simms, M., 1984, Dolomitisation by groundwater flow systems in carbonate platforms: Transactions of the Gulf Coast Association Geological Science, v. 24, p. 411-420.

Smalley, P.C., Malle, C.N., Coleman, M.L. and Roose, J.E., 1992, LASSIE (laser ablation sampler for stable isotope extraction) applied to carbonate minerals: Chemical Geology, v. 101, p. 43-52.

Smart, P.L., Palmer, R.J., Whitaker, F.F. and Wright, V.P., 1988, Neptunian dykes and fissure fills: an overview and account of some modern examples: in James, N.P. and Choquette, P.W., eds, Paleokarst, Springer-Verlag, New York, p. 149-163.

Vahrenkamp, V.C. and Swart, P.K., *in* press, Late Cenozoic sea-water generated dolomites of the Bahamas: metastable analogues for the genesis of ancient platform dolomites, in Purser, B., Tucker M. and Zenger D., eds, Dolomites: a volume in honor of Dolomieu, International Association of Sedimentologists.

Vahrenkamp, V.C., Swart, P.K. and Ruiz, J., 1991, Episodic dolomitisation of Late Cenozoic carbonates in the Bahamas: Evidence from strontium isotopes: Journal of Sedimentary Petrology, v. 61, p. 1002-1014.

Ward, W.C. and Halley, R.B., 1985, Dolomitisation in a mixing zone of near-seawater composition, Late Pleistocene, North-east Yucatan Peninsula: Journal of Sedimentary Petrology, v. 55, p. 407-420.

Whitaker, F.F., 1992, Hydrology, geochemistry and diagenesis of modern carbonate platforms in the Bahamas. PhD Thesis, Department of Geography, University of Bristol, UK, 347 p.

Whitaker, F.F. and Smart, P.L., 1990, Circulation of saline groundwaters through carbonate platforms; evidence from the Great Bahama Bank: Geology, v. 18, p. 200-204.

Whitaker, F.F. and Smart, P.L., *in* press, Circulation of saline groundwaters through carbonate build-ups; an overview and case study from the Bahamas: in Horbury, A. and Robinson, A., eds, Diagensis and Basin Development, American Association of Petroleum Geologists Memoir.

Whitaker, F.F., Smart, P.L., Vahrenkamp, V.C., Nicholson, H. and Wogelius, R.A., *in* press, Dolomitisation by near-normal sea water? Evidence from the Bahamas, in Purser, B. Tucker M. and Zenger D., eds, Dolomites: a volume in honor of Dolomieu, International Association of Sedimentologists.

Wogelius, R.A., Frasar, D.G., Feltham, D.J. and Whiteman, M.I., 1992, Trace element zoning in dolomite; Proton microprobe data and thermodynamic constraints on fluid composition: Geochimica Cosmochimica Acta, v. 56, p. 319-334.